Imaging of Zn2+ release from pancreatic beta-cells at the level of single exocytotic events. Anal Chem

ARTICLE *in* ANALYTICAL CHEMISTRY · JULY 2003

Impact Factor: 5.64 · Source: PubMed

3 AUTHORS, INCLUDING:

Wei-Jun Qian
Pacific Northwest National Laboratory
132 PUBLICATIONS **5,767** CITATIONS
SEE PROFILE

Kyle R Gee
Thermo Fisher Scientific
111 PUBLICATIONS **4,472** CITATIONS
SEE PROFILE

Anal. Chem. **2003,** *75,* 3468−3475

Imaging of Zn^{2+} Release from Pancreatic β-Cells at the Level of Single Exocytotic Events

Wei-Jun Qian,[†,‡] Kyle R. Gee,[§] and Robert T. Kennedy*[,†,∥]

Department of Chemistry and Department of Pharmacology, University of Michigan, Ann Arbor, Michigan 48109, and Molecular Probes, Inc., 4849 Pitchford Avenue, Eugene, Oregon 97402

Regulated secretion of Zn^{2+} from isolated pancreatic β-cells was imaged using laser-scanning confocal microscopy. In the method, β-cells were incubated in a solution containing the novel fluorescent Zn^{2+} indicator FluoZin-3. Zn^{2+} released from the cells reacted with the dye to form a fluorescent product, which was detected by the confocal microscope. The new dye is much brighter than Zinquin, previously used for this application, allowing detection limits of 10−40 nM and temporal resolution of 16 ms/image. The high temporal resolution allowed imaging of isolated fluorescent transients that occurred at the edge of the cells following stimulation with 20 mM glucose or 40 mM K^+. Fluorescent transients took 16−50 ms to reach a peak from the initial rise and returned to baseline after 170 ± 50 ms (n = 78 transients from 15 cells). It was concluded that the transients correspond to detection of exocytotic release of Zn^{2+}. Analysis of the temporal and spatial dispersion of the transients indicates that the release of Zn^{2+} is not diffusion limited but is instead kinetically controlled in agreement with previous observations of insulin release detected by amperometry.

Neurotransmitters and hormones are typically secreted from cells by exocytosis wherein vesicles containing signaling molecule fuse with the plasma membrane, thus allowing vesicular contents to enter the extracellular environment. Exocytosis results in release of attomole quantities or less within a few milliseconds making detection of this process a significant analytical challenge. The past 15 years have seen significant advances in the ability to detect and monitor secretion from live cells with sufficient sensitivity and temporal resolution to detect and resolve isolated exocytotic events. Methods include capacitance, amperometry, and fluorescence imaging. These methods have led to dramatic increases in our knowledge of the mechanism of secretion and intercellular communication. In capacitance measurements, increases in membrane capacitance associated with exocytosis are monitored with a pipet electrode clamped to the cell. Amperometry detects the actual released chemicals using a microelectrode positioned close to the cell surface. This method has been applied to several transmitter substances including catecholamines,[1] histamine,[2] melanocyte stimulating hormone,[3] and insulin.[4] A variety of imaging methods have also become available. Most of these methods utilize labeling of the vesicles using green fluorescent protein (GFP) fusion to a vesicle protein[5,6] or a dye that partitions into acidic compartments such as vesicles[7,8] and then observing vesicular transport within the cell. These methods allow individual vesicles to be tracked up to the point of fusion and in some cases detection of the released label. Alternatively, the membrane can be labeled using FM1-43, a dye that increases fluorescence upon partitioning into a lipophilic environment.[9] More recently, the penetration of a fluid-phase tracer into plasma membrane invaginations caused by vesicle fusion has been used to image exocytosis.[10]

Luminescence has also been used to directly monitor secreted substances as they are released from the cell.[11−15] In some cases, native fluorescence can be used to track the released substance;[11] however, in most of these methods, cells are bathed in a reagent that reacts with released molecules to form a luminescent product that is detected by an imaging method. Examples of this approach include monitoring ATP secretion using a chemiluminescent reaction[12] and monitoring of Zn^{2+} release using zinc indicators and fluorescence microscopy.[13,14] These methods are akin to amperometry in that they directly detect a native released

* Corresponding author. Phone: 734-615-4363. Fax: 734-615-6462. E-mail: rtkenn@umich.edu.

† Department of Chemistry, University of Michigan.

‡ Current address: Environmental and Molecular Sciences Laboratory, Pacific Northwest National Laboratory, P.O. Box 999, MSIN: K8-98, Richland, WA 99352.

§ Molecular Probes, Inc.

∥ Department of Pharmacology, University of Michigan.

(1) Wightman, R. M.; Jankowski, J. A.; Kennedy, R. T.; Kawagoe, K. T.; Schroeder, T. J.; Leszczyszyn, D. J.; Near, J. A.; Diliberto, E. J.; Viveros, O. H. *Proc. Natl. Acad. Sci. U.S.A.* **1991**, *88*, 10754−10758.

(2) Pihel, K.; Travis, E. R.; Borges, R.; Wightman, R. M. *Biophys. J.* **1996**, *71*, 1633−1640.

(3) Paras, C. D.; Kennedy, R. T. *Anal. Chem.* **1995**, *67*, 3633−3637.

(4) Huang, L.; Shen, H.; Atkinson, M. A.; Kennedy, R. T. *Proc. Natl. Acad. Sci. U.S.A.* **1995**, *92*, 9608−9612.

(5) Han, W.; Li, D.; Levitan, E. S. *Ann. N. Y. Acad. Sci.* **2002**, *971*, 627−633.

(6) Tsuboi, T.; Zhao, C.; Terakawa, S.; Rutter, G. A. *Curr. Biol.* **2000**, *10*, 1307−1310.

(7) Suzaki, E.; Kobayashi, H.; Kodama, Y.; Masujima, T.; Terakawa, S. *Cell Motil. Cytoskeleton* **1997**, *38*, 215−228.

(8) Schmoranzer, J.; Goulian, M.; Axelrod, D.; Simon, S. M. *J. Cell. Biol.* **2000**, *149*, 23−32.

(9) Betz, W. J.; Mao, F.; Bewick, G. S. *J. Neurosci.* **1992**, *12*, 363−375.

(10) Takahashi, N.; Kishimoto, T.; Nemoto, T.; Kadowaki, T.; Kasai, H. *Science* **2002**, *297*, 1349−1352.

(11) Lillard, S. J.; Yeung, E. S. *J. Neurosci. Methods* **1997**, *75* (1), 103−109.

(12) Wang, Z.; Haydon, P. G.; Yeung, E. S. *Anal. Chem.* **2000**, *72*, 2001−2007.

(13) Qian, W. J.; Aspinwall, C. A.; Battiste, M. A.; Kennedy, R. T. *Anal. Chem.* **2000**, *72*, 711−717.

(14) Gee, K. R.; Zhou, Z. L.; Qian, W. J.; Kennedy, R. T. *J. Am. Chem. Soc.* **2002**, *124*, 776−778.

(15) Thompson, R. B.; Whetsell, W. O.; Maliwal, B. P.; Fierke, C. A.; Frederickson, C. J. *J. Neurosci. Methods* **2000**, *96*, 35−45.

10.1021/ac0341057 CCC: $25.00
Published on Web 05/20/2003

substance. This allows study of the final stage of exocytosis, which is extrusion and dispersion of released product. In addition, they minimally perturb the cell. Thus, they can be used on primary cells and can be expected to have minimal impact on normal cell function. This is in contrast, for example, to the use of a GFP fusion, which requires genetic manipulation of the cells and in general must be performed on clonal cell lines. Until now, however, imaging of release products has not allowed the temporal resolution or sensitivity to detect isolated excocytotic events.

We have demonstrated the use of scanning confocal microscopy in combination with Zinquin to image Zn^{2+} released from individual pancreatic β-cells.[13,14] Zn^{2+} is co-localized with insulin within the vesicles of pancreatic islet cells[16] and co-released during exocytosis.[17−21] Within vesicles, Zn^{2+} is believed to stabilize the insulin crystals; however, its function upon release is still being elucidated. Zn^{2+} released from pancreatic β-cells may act as a paracrine agent in promoting islet cell death, especially in hyperinsulinemic states.[22] Secreted Zn^{2+} may also activate ATP-sensitive K^+ channels on β-cells and therefore serve an autoregulatory role in secretion.[23] Zn^{2+} is also stored and released from some glutmatergic neurons.[24] Free Zn^{2+} has been shown to influence a variety of receptors and ion channels[25] present on cell surfaces including NMDA[26] and GABA[27] receptors. These observations have led to the concept that Zn^{2+} is an atypical neurotransmitter.[28] Released Zn^{2+} may also play a role in the development of Alzheimer's disease and excitotoxicity.[29,30] Given the potential roles for released Zn^{2+} in modulating neuronal and endocrine functions, it would be of interest to better understand the regulation and dynamics of Zn^{2+} release from these cells.

Limitations of the Zinquin dye previously used for β-cell secretion imaging include a tendency to partition into the plasma membrane, requirement of excitation in the mid-UV range, which promotes cell damage, and relatively weak fluorescence. The latter limited temporal resolution for image acquisition to ~1 Hz.[13] In a preliminary study using FluoZin-3, we recently demonstrated that this dye has high selectivity for Zn^{2+} and greatly mitigates the problems of Zinquin in that it has undetectable penetration into the cell, is excited at 488 nm, and has much higher quantum yield than Zinquin.[14] In the present work, we evaluate the dye for high temporal resolution monitoring of Zn^{2+} release from pancreatic β-cells. We demonstrate that, when used with fast scanning confocal microscopy, the dye allows images of Zn^{2+} secretion to be acquired at 60 Hz, a rate high enough to observe isolated exocytotic events. It is anticipated that this method will be useful for fundamental studies of exocytosis in pancreatic β-cells.

EXPERIMENTAL SECTION

Chemicals. FluoZin-3 was prepared at Molecular Probes as previously described.[14] Tetrakis(2−pyridylmethyl)ethylenediamine (TPEN) was from Molecular Probes. Type XI collagenase, HEPES, and EGTA were from Sigma. Unless otherwise stated, all chemicals for islets and cell culture were obtained from Life Technologies. All other chemicals were from Fisher unless noted and were of the highest purity possible.

Isolation and in Vitro Culture of Mouse Pancreatic β-Cells. Pancreatic islets were isolated from CD-1 mice by ductal injection with type XI collagenase and were dispersed into isolated cells by shaking in 0.025% trypsin/EDTA for 6 min at 37 °C.[31] Dispersed cells were plated onto 25-mm-diameter coverslips in tissue culture dishes (Corning) and incubated in RPMI 1640 medium containing 10% fetal bovine serum, 100 units/mL penicillin, and 100 μg/mL streptomycin at 37 °C, 5% CO_2, pH 7.4. Cells were used for experiments 1−2 days after isolation.

Confocal Imaging. All imaging experiments were performed on a Nikon RCM 8000 confocal laser-scanning microscope with a Nikon 40×, 1.15 NA, UV-corrected water-immersion objective. This system acquires full field-of-view scan at a fixed rate of 30 Hz, i.e., 30 full frames/s. Scans can be averaged to reduce noise in an acquired image at the cost of temporal resolution. For example, 32 scans can be collected at 30 Hz and signal averaged to generate an image every 1.07 s. Image acquisition rates greater than 30 Hz can be achieved using band scanning mode. For example, for a two-band scanning mode, the original full frame is divided into two equal bands and only one band is scanned. Therefore, the image acquisition rate for this scan mode is 60 Hz, which is 2 times faster than that of full frame scanning (assuming no signal averaging).

Zn^{2+} images with FluoZin-3 were acquired with 488-nm excitation and 525 ± 10 nm band-pass emission filters. All images were stored on an optical disk cartridge (TQ-FH332, Panasonic) by an optical disk recorder (TQ-3038F, Panasonic) for later analysis. To create cell images shown in the figures, a cell was scanned for 1.07 s with 351-nm excitation, which produced an image of the cell based on autofluorescence. FluoZin-3 fluorescence images collected were then overlaid these images so that the fluorescence signal could be seen relative to the cell. Without the autofluorescence scan, the cells would not be visible because of the low background fluorescence.

Buffer with minimum background Zn^{2+} level was prepared as previously described for imaging experiments.[15] Briefly, Kreb's Ringer buffer (KRB: 118 mM NaCl, 5.4 mM KCl, 2.4 mM $CaCl_2$, 1.2 mM $MgSO_4$, 1.2 mM KH_2PO_4, 20 mM HEPES, 3.0 mM D-glucose) was prepared with all ingredients except calcium and magnesium salts. The buffer was then treated with Chelex-100 (Bio-Rad) for 2 h (5 g of Chelex-100/100 mL of buffer). The pH of the buffer was adjusted to 7.4 after Chelex-100 treatment and Puratronic grade $CaCl_2$ and $MgSO_4$ (Alfa Aesar) were added to

(16) Zalewski, P. D.; Millard, S. H.; Forbes, I. J.; Kapaniris, O.; Slavotinek, A.; Betts, W. H.; Ward, A. D.; Lincoln, S. F.; Mahadevan, I. B. *J. Histochem. Cytochem.* **1994**, *42*, 877−884.
(17) Emdin, S. O.; Dodson, G. G.; Cutfield, J. M.; Cutfield, S. M. *Diabetologia* **1980**, *19*, 279−402.
(18) Formby, B.; Schmid-Formby, F.; Grodsky, G. M. *Diabetes* **1984**, *33*, 229−234.
(19) Gold, G.; Grodsky, G. M. *Experientia* **1984**, *40*, 1105−1114.
(20) Grodsky, G. M.; Schmid-Formby, F. *Endocrinology* **1985**, *117*, 704−710.
(21) Foster, M. C.; Leapman, R. D.; Li, M. X.; Atwater, I. *Biophys. J.* **1993**, *64*, 525−532.
(22) Kim, B. J.; Kim, Y. H.; Kim, S.; Kim, J. W.; Koh, J. Y.; Oh, S. H.; Lee, M. K.; Kim, K. W.; Lee, M. S. *Diabetes* **2000**, *49*, 1325−1333.
(23) Bloc, A.; Cens, T.; Cruz, H.; Dunant, Y. *J. Physiol.* **2000**, *529*, 723−734.
(24) Huang, E. P. *Proc. Natl. Acad. Sci. U.S.A.* **1997**, *94*, 13386−13387.
(25) Harrison, N. L.; Gibbons, S. J. *Neuropharmacology* **1994**, *33*, 935−952.
(26) Peters, S.; Koh, J.; Choi, D. W. *Science* **1987**, *236*, 589−593.
(27) Smart, T. G.; Moss, S. J.; Xie, X.; Huganir, R. L. *Br. J. Pharmacol.* **1991**, *103*, 1837−1839.
(28) Baranano, D. E.; Ferris, C. D.; Snyder, S. H. *Trends Neurosci.* **2001**, *24* (2), 99−106.
(29) Cuajungco, M. P.; Lees, G. J. *Brain Res. Rev.* **1997**, *23*, 219−236.
(30) Frederickson, C. J.; Suh, S. W.; Silva, D.; Frederickson, C. J.; Thompson, R. B. *J. Nutr.* **2000**, *130*, 1471S-1483S.
(31) Pralong, W. F.; Bartley, C.; Wollheim, C. B. *EMBO J.* **1990**, *9*, 53−60.

the final concentrations. During all experiments and solution preparation, glass containers were avoided to minimize metal contamination. Even with these precautions, the Zn^{2+} level was estimated to be 200 nM by titration. This background free Zn^{2+} was depleted by chelation with TPEN as discussed below.

Cells to be imaged were bathed in 3 mL of KRB containing 2 μM FluoZin-3 and maintained at 37 °C on the stage of the microscope by a microincubator (Medical Systems, Inc.). Before imaging, the buffer was titrated with a high-affinity nonfluorescent Zn^{2+} chelator TPEN to deplete the trace amount of Zn^{2+} present in the buffer in order to reduce background fluorescence. The typical final concentration of TPEN in the buffer was ~200 nM. Stimulation (40 mM K^+ or 20 mM glucose) solutions containing the same concentration of FluoZin-3 as the bathing buffer were applied to the cells by continuous pressure ejection at 3−6 psi from micropipets positioned ~60 μm from the cells for the times indicated. In preliminary experiments, these conditions were shown to result in about 10−20 nL/10 s of buffer being ejected creating a homogeneous concentration over the cell clusters investigated.

Data Analysis. Images were played back from the optical disk cartridge and captured and analyzed using Simca image analysis software (C-Imaging Systems). For plots of fluorescence intensity as a function of time, regions of interest (ROIs) around the cells were highlighted and average intensities within the ROIs were calculated for a series of images. To convert fluorescence intensities into the total Zn^{2+} concentrations ($[Zn^{2+}]$), a two-point calibration was performed following each experiment, which gave the background fluorescence in the absence of Zn^{2+} (F_{min}) and the maximum fluorescence at saturated Zn^{2+} level (F_{max}). The total $[Zn^{2+}]$ was calculated using the following equation:

$$\text{total } [Zn^{2+}] = \text{total } [\text{FluoZin} - 3](F - F_{min})/(F_{max} - F_{min}) \quad (1)$$

where F is measured fluorescence intensity at a given $[Zn^{2+}]$. All means are reported as ±1 standard deviation.

RESULTS AND DISCUSSION

Imaging of Zn^{2+} Release with FluoZin-3. In initial experiments, 32 scans were averaged to obtain 1.07-s temporal resolution similar to what had been used for Zinquin. A titration calibration with $ZnCl_2$ under these conditions yielded a detection limit of 10 nM, which was a 50-fold improvement over that obtained using Zinquin. This improvement is attributed to greater sensitivity of the dye and lower background autofluorescence from both the cell and surrounding solution due to the longer wavelength for excitation.

Images of cells during stimulation with 40 mM K^+ and 20 mM glucose under these conditions are shown in Figure 1. As expected and previously demonstrated,[13,14] large fluorescent increases are observed at the cell periphery that persist for several seconds following stimulation. These signals correspond to detection of Zn^{2+} co-released with insulin. The imaging technique allows visualization of the clouds of Zn^{2+} as they form and then diffuse away from the cell. Released Zn^{2+} can be detected at least 20 μm away from the cell surface, while in previous work with Zinquin, Zn^{2+} was only detected in the immediate vicinity of the cell (1−2 μm away from the cell surface). As previously reported,[14] this dye has undetectable penetration into the cell (unlike Zinquin) presumably because of the three negative charges on the molecule at physiological pH. The resulting low background from the cell and membrane aids detection.

Imaging of Zn^{2+} Release with High Temporal Resolution. Although the Zn^{2+} detected in Figure 1 was released by exocytosis, which should result in rapid fluctuations in signal, the temporal resolution was too low to observe such fast changes, which are expected to occur in milliseconds. As a result, the signal appears as a relatively smooth curve. We therefore evaluated the possibility of imaging at 16-ms intervals (60 Hz) using two-band scanning (see Experimental Section) and no signal averaging. (The instrument used for these experiments does not allow signal averaging in the band scanning mode.) The detection limit for total $[Zn^{2+}]$ was 40 nM under these conditions. This 4-fold degradation of detection limit relative to that obtained at 1-s temporal resolution (32 scans averaged) is close to the 5-fold theoretically expected for bypassing signal averaging.

Figure 2 illustrates detection of Zn^{2+} release at the higher acquisition rate. As shown by the traces, within certain locations around a cell, distinct fluorescence transients with durations between 100 and 300 ms were observed whereas no signal was recorded at other regions. These highly localized sharp changes in $[Zn^{2+}]$ are presumably due to the release of Zn^{2+} in packets from individual secretory vesicles by exocytosis. The montage in Figure 2 shows a series of images corresponding to the marked fluorescence spike, which has a total duration of ~150 ms. Although the images are much noisier than those acquired at lower temporal resolution due to the lack of signal averaging, it is possible to clearly observe the appearance, growth, and dissipation of the Zn^{2+} cloud over the 150-ms time span of the montage. Isolated Zn^{2+} release events similar to those shown in Figure 2 were observed in 15 separate experiments when cells were stimulated by 40 mM K^+ or 20 mM glucose. (In all these experiments, either single cells or cell clusters consisting of two to five cells were used.) The remarkable isolation of the spikes to individul portions of the cell membrane, an indication of a "hot spot", is in agreement with previous observations by our group and others.[10,13,32] As previously observed, these hot spots were not correlated to the position of the pipet and appeared to be fixed on the cell.[32,33]

Identification of Release Sites. The spatial and temporal aspects of the isolated spikes were further examined to evaluate the utility of this method. Although diffusion of released Zn^{2+} leads to the detection of a large Zn^{2+} cloud, the most concentrated Zn^{2+} signal should appear at the site of exocytosis, thus allowing a precise location of the site of release. To determine whether it was possible to detect differences in intensity associated with a single fluorescence spike, 2-μm-square ROIs along the cell surface were analyzed as shown in Figure 3. Clear differences in intensity and width are seen with the different ROI's. The narrowest and highest amplitude trace is from ROI 3, suggesting that the release site is localized within this region. As regions removed from the release site (ROI 3) either laterally (sites 1, 2, 4, and 5) or normally

(32) Paras, C. D.; Qian, W. J.; Lakey, J. R. T.; Tan, W. H.; Kennedy, R. T. *Cell Biochem. Biophys.* **2000**, *3*, 227−240.
(33) Qian, W. J.; Kennedy, R. T. *Biochem. Biophys. Res. Commun.* **2001**, *286*, 315−221.

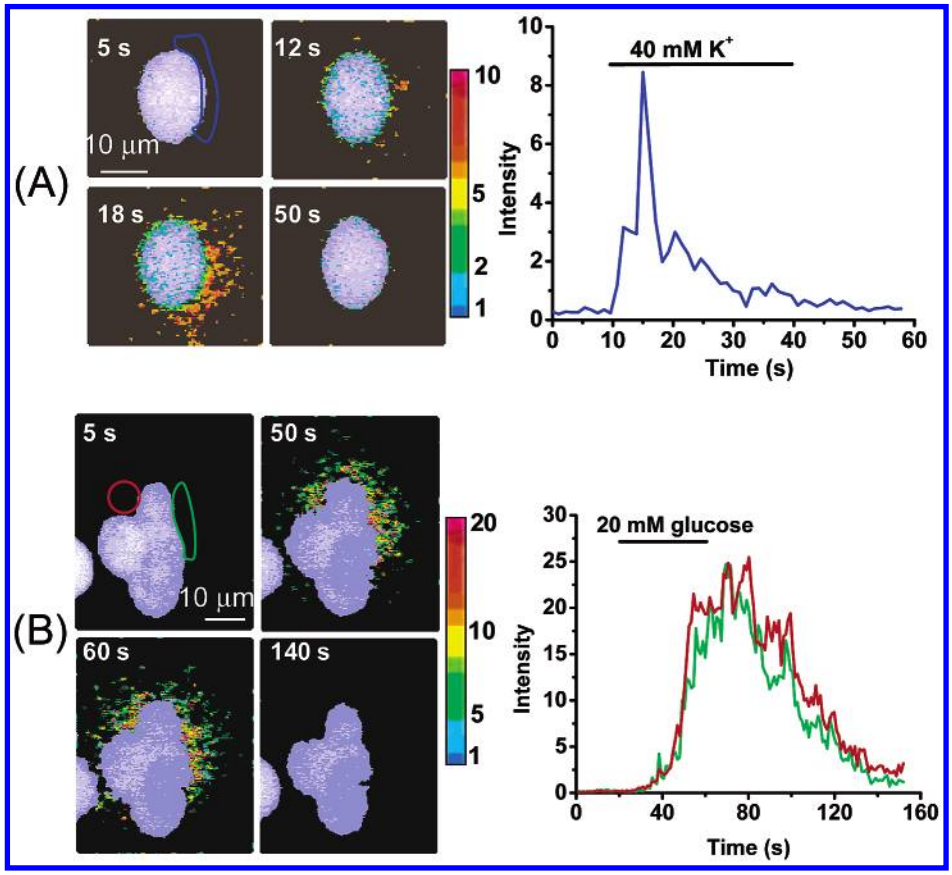

Figure 1. Imaging of Zn^{2+} release from isolated pancreatic β-cells at 1-s temporal resolution. Images are shown in fluorescence intensity ratios against a UV autofluorescence image in order to highlight the extracellular fluorescence enhancements. Fluorescence intensity ratio was color coded as indicated by the scale bars. The time at which each image was acquired is indicated in seconds. All images were acquired at a rate of 1 Hz (32 scans averaged/image). The temporal responses were analyzed using ROIs outside the cells as indicated in the images. The bars on top of the traces indicate the periods of stimulation. (A) Zn^{2+} release from a single cell induced by 40 mM K^+ stimulation. (B) Zn^{2+} release from a cluster of four cells induced by 20 mM glucose stimulation. The temporal responses were analyzed from the two ROIs shown in the left image, and each data trace corresponds to the ROI with the same color.

(sites 6 and 7), the detected fluorescence spikes are broader and with lower peak [Zn^{2+}], consistent with the diffusional transport of released Zn^{2+} away from the site of release. Thus, the release site can readily be localized to a single 2-μm square on the cell surface.

Conversion to Concentration. Because of the high Zn^{2+} affinity of FluoZin-3 and 1:1 FluoZin-3−Zn^{2+} binding,[14] the fluorescence signal is expected to be proportional to the [Zn^{2+}] present in the extracellular space if the total [Zn^{2+}] is less than the total FluoZin-3 concentration. Therefore, fluorescence intensities can be converted into the total [Zn^{2+}] using eq 1. Using this approach, the average peak concentration was found to be 150 ± 95 nM (n = 78 spikes from 15 cells) at the release site. Thus, with certain caveats discussed below, the imaging technique can provide an estimate of the actual concentration that would be present at the cell surface, which is important for investigation of potential transmitter interactions with receptor.

Mapping the concentrations around a release site can be used to estimate the amount of Zn^{2+} released per exocytotic event. As shown in Figure 2, the Zn^{2+} forms a semicircular cloud extending from the cell. As this image represents a slice taken through the cell and surrounding space, it is reasonable that the released Zn^{2+} occupies a hemisphere with a radius defined by the extent of detectable signal (~6 μm at 49 ms in Figure 2). Multiplying the average concentration within a slice seen in an image by the volume of the corresponding hemisphere yields an average of 0.2 ± 0.1 amol of free Zn^{2+}/event (n = 6). Previous estimates of the amount of insulin released per exocytotic event were 1.6 amol.[4] Zn^{2+} is believed to be stored in a complex with insulin at a ratio of 6 insulin/2 Zn^{2+} leading to a prediction that the free Zn^{2+} released should be 1/3 of the free insulin released or 0.5 amol of Zn^{2+}/vesicle. Therefore, based on the previously detected insulin content of vesicles, the detected free Zn^{2+} level is somewhat lower than expected. If this determination is accurate, then it is reasonable to conclude that not all insulin has bound Zn^{2+} in the expected ratio, resulting in less Zn^{2+} level per exocytotic event than expected. However, it is also possible that the low estimate is an artifact of the measurement. In particular, if Zn^{2+} that was released during exocytosis remained bound to insulin or was bound by TPEN in solution (TPEN was added to reduce the background, see Experimental Section), then it could diffuse away from the cell without being bound by FluoZin-3 and escape detection. In addition, free Zn^{2+} could diffuse away from the cell without having time to react with the Fluo-Zin3; however, this seems unlikely as a preliminary experiment in which Zn^{2+} and Fluo-Zin3 were rapidly mixed, ejection from micropipets while monitoring on the microscope revealed that the reactions were completed in <16 ms.

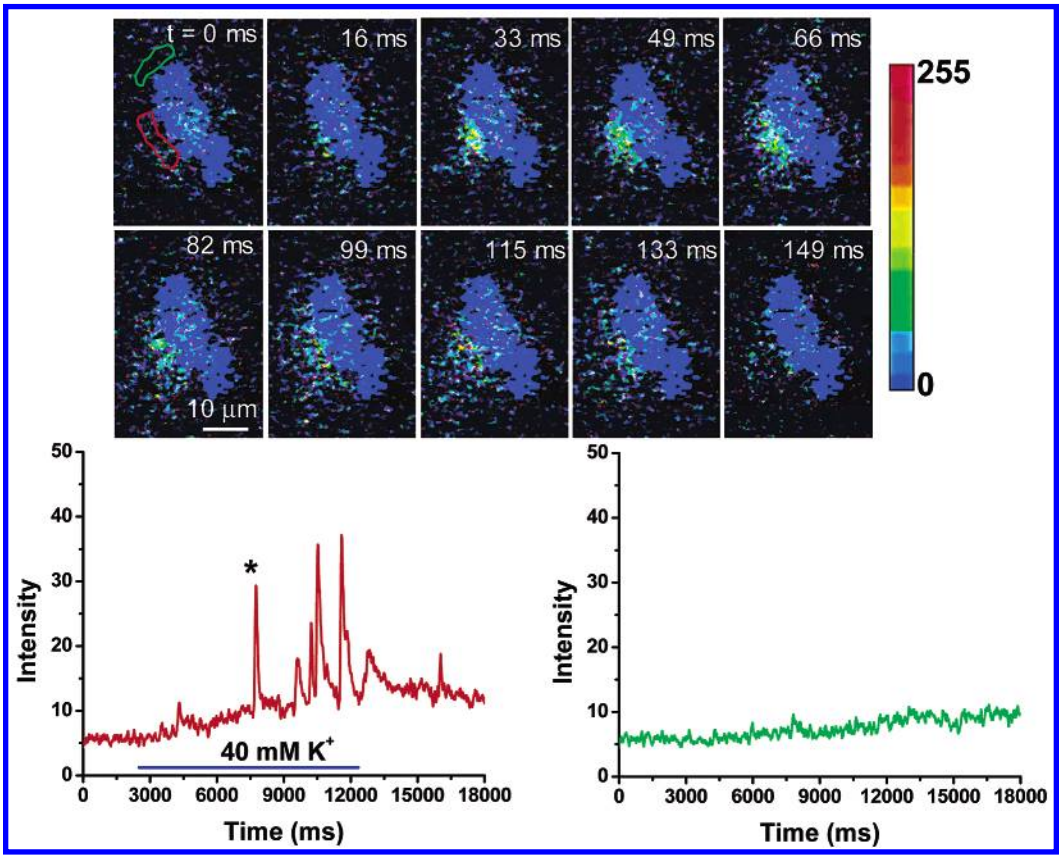

Figure 2. Detection of Zn^{2+} release with 16-ms temporal resolution. A cluster of three cells was stimulated by 40 mM K^+ for 10 s, and images were acquired continuously at a rate of 16.5 ms/image (60 Hz, two-band scanning). Images shown are in raw intensities pseudocolored according to the scale bar. The time courses of Zn^{2+} release were analyzed using the two ROIs outside the cells as shown in the first image. The traces in the bottom plots correspond to the ROIs in the same color. Images in the montage show the same fluorescence burst as the one marked with an asterisk in the bottom plot.

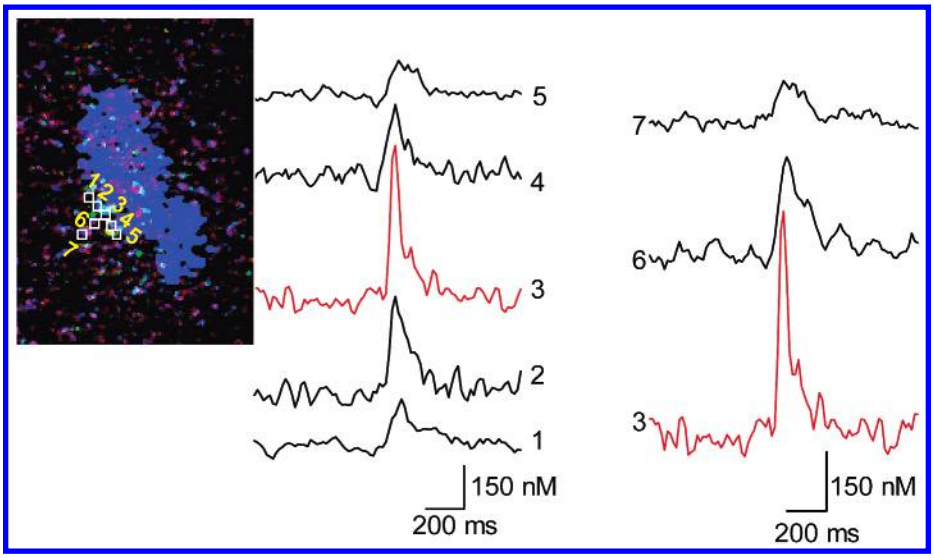

Figure 3. Identification of the release site of a single release event. The release event analyzed was the same as the one in Figure 2 marked with an asterisk. Seven identical ROIs were aligned outside the releasing area with the ROIs 1−5 lying against the cell surface and ROIs 6 and 7 moving away from the cell. The time courses of Zn^{2+} release from all regions are plotted on the same time scale. The amplitudes of the spikes are indicated as total [Zn^{2+}] in nanomolar.

Resolution of Closely Spaced Spikes. The spatial and temporal resolution of this technique also allows resolution of events that occur nearly simultaneously but at different sites on the cell. Figure 4 illustrates two release events that occurred within 300 ms of each other but were from two release sites ~8 μm apart. When data were analyzed using a relatively large ROI covering both release sites (trace 1), the fluorescence spike appears to be resulting from a single release event with a relatively broad peak; however, when data were analyzed by several small ROIs along the release site (traces 2−4), two peaks, corresponding to two

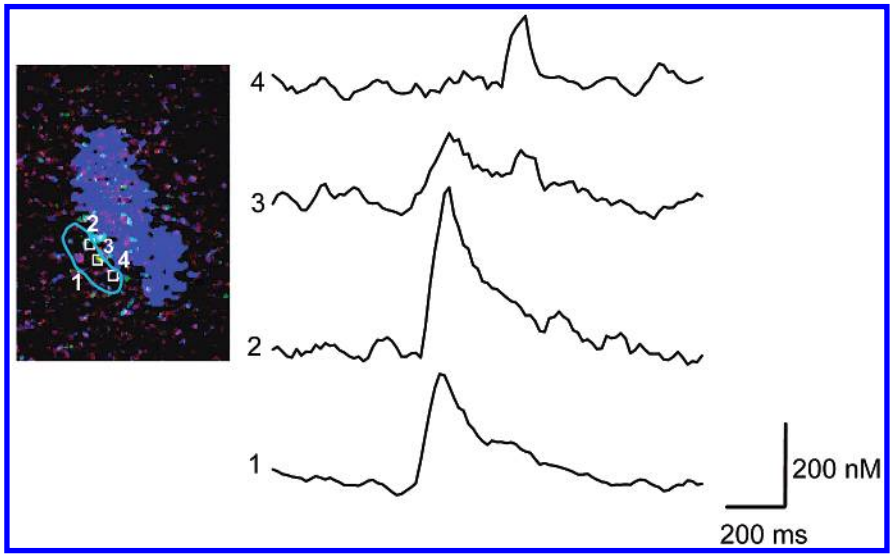

Figure 4. Spatially resolved analysis of temporally overlapped fluorescence spikes. Traces show the temporal change in detected concentration in one large ROI (1) and three smaller ROIs (2−4) taken from the same cell as shown in the image. The diameter of the small square region is 2 μm. Images were acquired at 60 Hz.

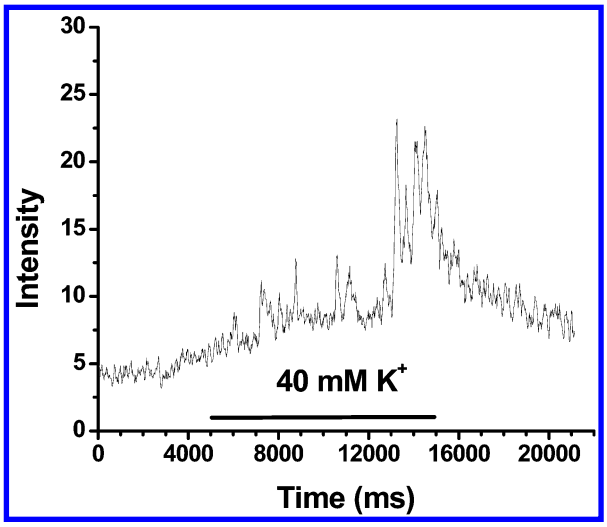

Figure 5. Fluorescence spikes evoked by K^+ stimulation. The cell was stimulated with K^+ for 10 s, and images were acquired at 60 Hz. Images were analyzed using an ROI around the release site as in Figure 2.

individual release events, were resolved and identified. The imaging technique, therefore, provides additional resolving power for temporally overlapped release events. In contrast, such temporally overlapped exocytotic events may not be resolved by single-point sensors such as microelectrodes used in amperometric measurements of exocytosis.

Even with the resolution of this method, it may be speculated that the observed spikes are not due to a single isolated exocytotic event. However, it has previously been shown that, with the low frequency of events detected, the probability of multiple release events occurring at the same release site within such small intervals (200 ms) is low if the exocytotic process is stochastic.[1]

Figure 5 shows an example of observation of multiple fluorescence spikes from a cell stimulated by K^+. Some of the spikes are not baseline resolved, and it is difficult to determine whether each spike corresponds to the detection of one single release event or multiple release events by only examining the temporal trace. By using smaller ROIs to map the release site similar to that in Figure 4, it was found that the observed fluorescence spikes were results of at least 22 independent release events. Beside the observation of multiple spikes, a slow increase in baseline intensity was also observed following the stimulation, indicating an increase in Zn^{2+} level around the cell. This slow increase in Zn^{2+} level may be due to the overlapping of multiple exocytotic events. Zn^{2+} release that originated below or above the focal plane may also contribute to this slow increase in signal.

Temporal and Spatial Characteristics of Isolated Release Events. The spatial and temporal characteristics of the fluorescence spikes were investigated in order to further evaluate the information content of this technique. Figure 6A shows examples of isolated fluorescence transients from five different cells. All spikes show a relatively fast rise in total [Zn^{2+}] followed by a slow decay, which is expected for rapid exocytotic release followed by diffusion of the release products from the site of fusion.[34] The rise times, defined as the time between the initiation and the peak of the transient, varied from 16 to 50 ms while the average spike duration was 175 ± 50 ms (n = 78 spikes from 15 different cells). (In this analysis, only well-resolved spikes with signal-to-noise ratio of >3 were used and all analysis was performed using a 2-μm-square ROI at the release site.) The temporal resolution of these measurements is 16 ms, which prevents accurate measurements of the rise time.

The Zn^{2+} transients detected by this approach can be compared to those observed for insulin by amperometry from the same cell type.[35,36] Despite the lower temporal resolution for the imaging, the observed rise times are in good agreement with those measured by amperometric detection of insulin, which gives the typical rise times of 25−40 ms. In previous amperometric measurements, the total duration of insulin spikes was longer at

(34) Schroeder, T. J.; Jankowski, J. A.; Kawagoe, K. T.; Wightman, R. M.; Lefrou, C.; Amatore, C. *Anal. Chem.* **1992**, *64*, 3077−3083.
(35) Aspinwall, C. A.; Brooks, S. A.; Kennedy, R. T.; Lakey, J. R. T. *J. Biol. Chem.* **1997**, *272*, 31308−31314.
(36) Kennedy, R. T.; Huang, L.; Aspinwall, C. A. *J. Am. Chem. Soc.* **1996**, *118*, 1795−1796.

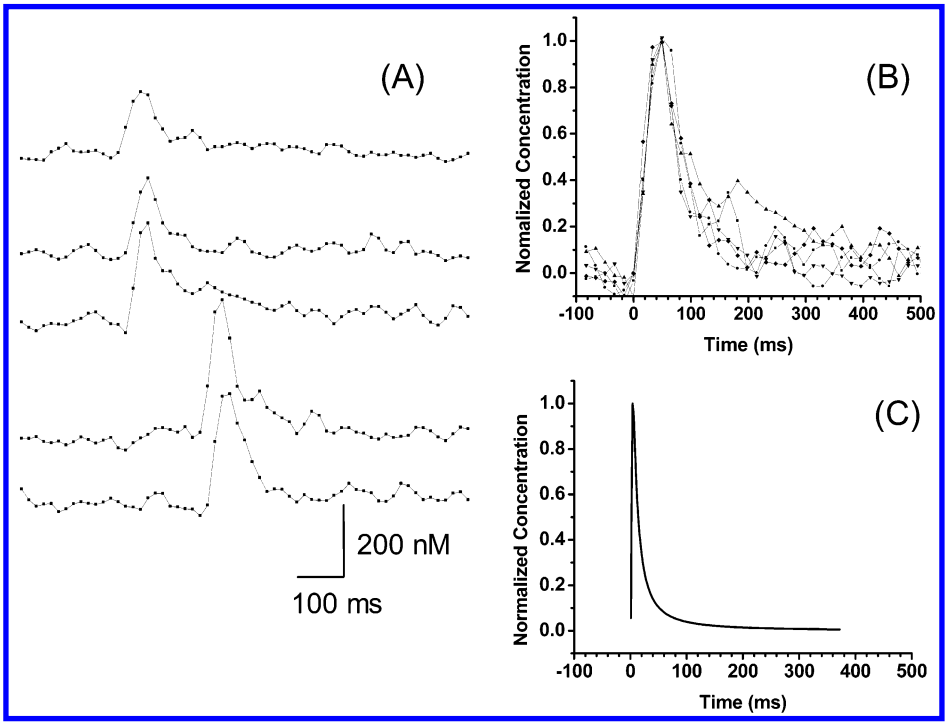

Figure 6. Shapes of isolated fluorescence spikes. (A) Examples of isolated fluorescence spikes obtained from five different cells. In all experiments, images were recorded at 60 Hz. The release sites of all release events were identified similarly as that in Figure 3, and each spike shown here was analyzed from a region close to the release site. The interval between two adjacent data points in the traces is 16 ms. (B) Spikes from (A) normalized by the peak [Zn^{2+}] and superimposed on the same time scale. (C) Diffusion-controlled spike based on the instantaneous point source diffusion model (eq 2) for a spot 3 μm away from the point source.

270 ± 165 ms.[4,36] The difference between the observed durations could be due to several differences in the experiments. The slower diffusion of insulin relative the Zn^{2+}/dye complex may result in a broader peak shape for the amperometric data. In addition, an amperometric sensor could detect an exocytotic event that occurred from a more distal location (such as near the bottom of a cell if the electrode is positioned on top of the cell).[37] In contrast, all of the fluorescence spikes are known to originate within the 2-μm ROI used for measurement.

Normalization of the five transients in Figure 6A to the peak signal and superimposition reveals that they have nearly identical temporal characteristics (Figure 6B). To determine whether the development of the transient was governed by diffusion, the observed shapes were compared to a diffusion-controlled model in which Zn^{2+} release was considered as diffusion from an instantaneous point source on a planar surface into a semi-infinite medium.[34,37] At any given time (t), the concentration at a distance r from an instantaneous point source into a semi-infinite medium is given by[38]

$$C(r,t) = \frac{M}{4(\pi Dt)^{3/2}} \exp(-r^2/4Dt)$$

$$= C(0,t) \exp(-r^2/4Dt) \qquad (2)$$

where C is the concentration of diffusing substance, the FluoZin-3−Zn^{2+} complex in this case, D is the diffusion coefficient, and M is the amount of substance (Zn^{2+}) released at $t = 0$. In these calculations, D for FluoZin-3−Zn^{2+} complex was taken as 3.4×10^{-6} cm^2/s, the value measured for fluorescein-labeled biotin, a compound with a molecular weight similar to that of the FluoZin-3−Zn^{2+} complex, in an aqueous solution.[39] Figure 6C shows a calculated spike shape, normalized to a peak value of 1, based on this model (eq 2). The model predicts a much narrower spike (rise time of 4 ms and total peak duration of ~60 ms) for a peak analyzed at 3 μm away from the point source than what was observed.

Since confocal imaging collects signals from ~1-μm-thick slice through the cell and the focal plane is typically positioned in the middle of the cell, it is possible that the actual release sites are located below or above the focal plane. However, the spikes selected for this analysis were with the narrowest shapes and the largest amplitudes. Therefore, it is reasonable to assume that the release spot is close to the focal plane and the distance between the point of analysis and the actual release point is 1−3 μm for these observed spikes. The measured rise times may be distorted by the acquisition rate; however, the large difference in the total duration leads to the conclusion that the release process is not limited by diffusion but instead is kinetically controlled.

Besides the temporal characteristics, the imaging method also allows the spatial characteristics of individual release events to be examined. In Figure 7, the profiles of total Zn^{2+} concentrations along a line normal to the cell were plotted for three different points of time during a single release event. The concentration profiles were compared to those predicted by the instantaneous

(37) Jankowski, J. A.; Schroeder, T. J.; Ciolkowski, E. L.; Wightman R. M. *J. Biol. Chem.* **1993**, *268*, 14694−14700.

(38) Crank, J. *The Mathematics of Diffusion*; Oxford University Press: Oxford, U.K., 1975.

(39) Kamholz, A. E.; Schilling, E. A.; Yager, P. *Biophys. J.* **2001**, *80*, 1967−1972.

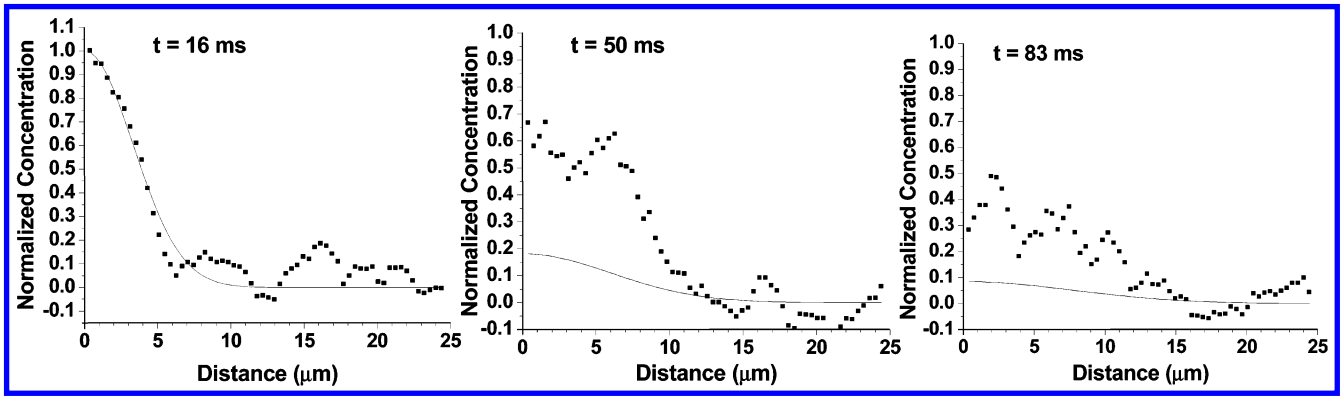

Figure 7. Normalized concentration profiles at different times during a single exocytotic release event. The release event analyzed is the same as shown in the montage of Figure 2. The image of first observation of the released Zn^{2+} cloud was assigned as $t = 16$ ms (the third image in the montage). The data points correspond to detected Zn^{2+} concentrations along a line starting from the release point away from cell surface. The concentrations were normalized against the maximum concentration measured at the release spot and $t = 16$ ms. Images used for analysis were smoothed with a 5×5 kernel in order to reduce the pixel-to-pixel noise in the images. All calculated curves were calculated from eq 2 based on the instantaneous point source diffusion model and normalized against $C(0, t_0)$, where $t_0 = 16$ ms. The correlation coefficient (R^2) of the fitting is 0.93 for $t = 16$ ms.

point source diffusion model (eq 2). The curves were normalized to achieve the maximal signal at the initial time point (16 ms), and then the model was used to predict the change based on diffusion at 50 and 83 ms. As time increases, both the measured and calculated concentration profiles display a decrease in amplitude and a broadening in shape; however, the decrease in amplitude for the calculated curves is much greater than that actually observed. For example, for the calculated curves, the maximum concentration at distance 0 and t =50 ms is 5.5-fold less than that at $t = 16$ ms. In contrast, the measured concentration at distance 0 and $t = 50$ ms is only 1.4-fold less than that at $t = 16$ ms. Therefore, the diffusion model predicts a much faster decrement in signal at the surface than what is actually observed. Thus, this examination of data also produces the conclusion that the Zn^{2+} release is not an instantaneous, diffusion-limited process.

This observation of kinetically controlled Zn^{2+} release is in agreement with the conclusion reached previously in an amperometric study on insulin release from these cells. We previously demonstrated that the dissolution and dissociation of the solid $(insulin)_6-(Zn^{2+})_2$ complex limits the escape of insulin from the cell during exocytosis. Thus, it is expected that detection of Zn^{2+} would also be kinetically controlled. Rate-limited extrusion of hormone has also been observed in adrenal chromaffin cells.[40]

Comparison to Amperometry. The work presented here provides the first temporally resolved measurements of chemical release resulting from individual exocytotic events by fluorescence imaging. Previously, only amperometry or voltammetry has provided the sensitivity and temporal resolution to monitoring chemical secretion from single cells at the level of single exocytotic events.[1,4,41,42] As a technique for monitoring exocytosis, this imaging approach appears to be complementary to amperometry. Amperometry maintains an advantage in temporal resolution and signal-to-noise ratio for detecting events. In addition, it more readily provides quantative information on the amount released by virtue of the relationship between charge passed and moles detected (Faraday equation). Finally, amperometry has been applied to several electroactive species while the fluorescence method is presently limited to Zn^{2+}. The fluorescence method, however, provides spatially resolved details that allow localization of secretory events (Figure 3), resolution of events that might be overlapping by a single-point sensor (Figure 4), and direct mapping of the concentration profiles that result following secretion (Figure 7). The latter information, while used here to demonstrate the kinetics of release, could be especially important in fundamental studies of receptor activation following secretion.

CONCLUSIONS

The use of FluoZin-3 in combination with fast-scanning confocal microscopy has been used to image secretion of Zn^{2+} from isolated pancreatic β-cells at 60 Hz. The combination of temporal and spatial resolution possible with the high-sensitivity dye allowed individual exocytotic events to be resolved. The Zn^{2+} is released over a time longer than expected for diffusion consistent with observations of insulin release made by amperometry. Future work will involve application of this method to other cells, such as Zn^{2+}-secreting neurons. In addition, further exploration of other dyes and luminescent methods may allow this method to be applied to other secretory systems.

ACKNOWLEDGMENT

This work is supported by NIH (DK 46960). W.-J.Q. received support as an ACS Division of Analytical Chemistry Fellow sponsored by Procter & Gamble.

Received for review February 3, 2003. Accepted April 24, 2003.

AC0341057

(40) Wightman, R. M.; Troyer, K. P.; Mundorf, M. L.; Catahan, R. *Ann. N. Y. Acad. Sci.* **2002**, *971*, 620−626.
(41) Chow, R. H.; von Ruden, L.; Neher, E. *Nature* **1992**, *356*, 60−62.
(42) Chen, T. K.; Luo, G.; Ewing, A. G. *Anal. Chem.* **1994**, *66*, 3031−3035.